

Finite and Infinite Population Spatial Rock-Paper-Scissors in One Dimension

Christopher Griffin ^{*‡}

Riley Mummah[†]

Russ deForest [‡]

June 5, 2022

Abstract

We derive both the finite and infinite population spatial replicator dynamics as the fluid limit of a stochastic cellular automaton. The infinite population spatial replicator is identical to the model used by Vickers and our derivation justifies the addition of a diffusion to the replicator. The finite population form generalizes the results by Durrett and Levin on finite spatial replicator games. We study the differences in the two equations as they pertain to the one-dimensional rock-paper-scissors game. In particular, we show that a constant amplitude traveling wave solution exists for the infinite population case and show how population collapse prevents its formation in the finite population case. This is closely related to recent work by Postlethwaite and Rucklidge on traveling waves in a similar but distinct rock-paper-scissor setting. Additional solution classes in variations of rock-paper-scissors are also studied.

1 Introduction

Evolutionary games using the replicator dynamic have been studied extensively and are now well documented [1–4]. Variations on the classical replicator dynamic include discrete time dynamics [5] and mutations [6, 7]. Additional evolutionary dynamics, such as imitation [1, 4, 8, 9] and exchange models [10] have been studied. Alternatively evolutionary games have been extended to include spatial models by a number of authors [11–18]. Most of these papers append a spatial component to the classical replicator dynamics (see e.g., [16]) or discuss finite population replicator dynamics in which total population counts are used (see e.g., [11]). In the latter case, a spatial term is again appended to the classical replicator structure.

In [19], Durrett and Levin study discrete and spatial evolutionary game models and compare them to their continuous, aspatial analogs. For their study the authors focus on a specific class of two-player two-strategy games using a hawk-dove payoff matrix. Because their payoff matrix is 2×2 , a single (spatial) variable $p(x, t)$ can be used to denote the proportion of the population playing hawk (Strategy 1) while a second variable $s(x, t)$ denotes the total population. Using the payoff matrix:

$$\mathbf{A} = \begin{bmatrix} a & b \\ c & d \end{bmatrix},$$

^{*}Applied Research Laboratory, Penn State University, University Park, PA 16802

[†]Department of Ecology and Evolutionary Biology, UCLA, Los Angeles, CA 90095

[‡]Department of Mathematics, Penn State University, University Park, PA 16802

the remarkable reaction-diffusion equation is analyzed:

$$\frac{\partial p}{\partial t} = \Delta p + \frac{2}{s} \nabla p \cdot \nabla s + pq((a-c)p + (b-d)(1-p)) \quad (1)$$

$$\frac{\partial s}{\partial t} = \Delta s + s(ap^2 + (b+c)p(1-p) + (1-p)^2d) - \kappa s^2. \quad (2)$$

Here κ is a death rate due to overcrowding and $q = (1-p)$. Let $\mathbf{e}_i \in \mathbb{R}^n$ be the i^{th} unit vector. Let $\mathbf{u} = \langle p, q \rangle$. When $\kappa = 0$, we can rewrite these equation as:

$$\frac{\partial p}{\partial t} = \Delta p + \frac{2}{s} \nabla p \cdot \nabla s + p(\mathbf{e}_1^T - \mathbf{u}^T) \mathbf{A} \mathbf{u} \quad (3)$$

$$\frac{\partial s}{\partial t} = \Delta s + s \cdot \mathbf{u}^T \mathbf{A} \mathbf{u}. \quad (4)$$

That is, Durrett and Levin have encoded the replicator dynamic into a finite population spatial partial differential equation, which differs from the one used by Vickers [16] because it assumes a finite population in its derivation.

In this paper we show that Durrett and Levin's finite population spatial replicator is generalizable to an arbitrary payoff matrix. We then focus our attention on the one-dimensional rock-paper-scissors game, which has interesting properties in both the finite and infinite population cases. In particular, we show: (i) the model used by Vicker's [16] arises naturally as the infinite population limit of the generalization of Durrett and Levin's model, which in turn can be derived from a stochastic cellular automaton (particle) model as a fluid limit, and (ii) the one dimensional infinite population spatial rock-paper-scissors dynamic has a constant amplitude traveling wave solution for all time. However, the finite population version does not exhibit such solutions, but does seem to exhibit an attracting stationary solution. We illustrate the latter result numerically.

2 Other Related Work

A portion of work in this paper (starting in Section 6) is focused on a comparison of the differences in finite and infinite population behaviors in the spatial replicator for Rock-Paper-Scissors (RPS). A substantial amount of work has been done on RPS, not all of which maps conveniently to results on the replicator dynamic or its spatial variants [20–28]. The earliest work to study competition among three species with cyclic dominance may be [24], which is contemporary but does predate the earliest work in evolutionary game theory (see e.g., [29–32]). In the past twenty years, there has been substantial work on the spatial dynamics of RPS that is independent of the spatial replicator dynamic [11–18]. Work till 2014 is reviewed in [22]. Mobility in cyclic competition (RPS) is studied in [23, 25]. The impact of reaction rates on spatial RPS is considered in [26], while the emergence of spiraling waves is studied in [21, 28]. More recently, traveling waves, spirals and heteroclinic bifurcations have been studied in [20, 27]. A discrete time model displaying chaos is considered in [33].

The results most closely related to those in this paper (specifically Section 7) can be found in the pair of papers by Postlethwaite and Rucklidge [20, 27]. Both these papers study a traveling wave solution for a specific spatial model of the rock-paper-scissors, with a more formal treatment given in [20]. The motivating aspatial model is given by the system of equations:

$$\dot{a} = a(1 - (a + b + c) - (\sigma + \zeta)b + \zeta c) \quad (5)$$

$$\dot{b} = b(1 - (a + b + c) - (\sigma + \zeta)c + \zeta a) \quad (6)$$

$$\dot{c} = c(1 - (a + b + c) - (\sigma + \zeta)a + \zeta b) \quad (7)$$

The observation is made that when $\sigma = 0$, this system exhibits the conserved quantities $a+b+c = 1$ and $abc = K$ for some constant K . Letting $u_1 = a$, $u_2 = b$ and $u_3 = c$, then Eqs. (5) to (7) can be written as the standard replicator:

$$\dot{u}_i = u_i \left((\mathbf{e}_i - \mathbf{u})^T \mathbf{A} \mathbf{u} \right), \quad (8)$$

where:

$$\mathbf{A} = \begin{bmatrix} -1 & -\zeta - 1 & \zeta - 1 \\ \zeta - 1 & -1 & -\zeta - 1 \\ -\zeta - 1 & \zeta - 1 & -1 \end{bmatrix} \quad (9)$$

This is trivially diffeomorphic to the replicator dynamic with payoff matrix:

$$\tilde{\mathbf{A}} = \zeta \begin{bmatrix} 0 & -1 & 1 \\ 1 & 0 & -1 \\ -1 & 1 & 0 \end{bmatrix}. \quad (10)$$

This is a scaled version of the standard (unbiased) RPS payoff matrix. However, when $\sigma \neq 0$, then Eqs. (5) to (7) can be written as:

$$\dot{u}_i = u_i \left(1 + \mathbf{e}_i^T \mathbf{B} \mathbf{u} \right), \quad (11)$$

with:

$$\mathbf{B} = \begin{bmatrix} -1 & -\sigma - \zeta - 1 & \zeta - 1 \\ \zeta - 1 & -1 & -\sigma - \zeta - 1 \\ -\sigma - \zeta - 1 & \zeta - 1 & -1 \end{bmatrix}. \quad (12)$$

Population evolution equations of this form are considered in [34]. When $\sigma = 0$, then $\mathbf{u}^T \mathbf{B} \mathbf{u} = \mathbf{u}^T \mathbf{A} \mathbf{u} = -1$, from which we derive Eq. (8). For $\sigma \neq 0$, this is not the case and consequently the dynamics of Eqs. (5) to (7) are not trapped on the unit 2-simplex as will be the case when we study (un)biased spatial replicator dynamics in finite and infinite populations. To be clear, the authors of [20,27] make no claim to this effect, however it does create an important distinction between the work in these papers and the work in this paper.

This does not mean the results in [20,27] are irrelevant to the discussion in Section 7. They are particularly relevant because when we follow a similar argument structure to those in [20,27], we find a similar traveling wave solution (as expected). Because our analysis is focused on the replicator dynamic, in both finite and infinite populations, the results, analysis and comparison are distinct from prior results and should be combined with those results in [21–28] (especially [20]) to provide a more complete picture of these unique cyclic dynamics of spatial rock-paper-scissors.

3 Model

Let $\mathbf{A} \in \mathbb{R}^{n \times n}$ be a payoff matrix for a symmetric game [4]. All vectors are column vectors unless otherwise noted. Below we construct a stochastic cellular automaton and show that the fluid limit of this system yields a generalization of Durrett and Levin’s specific finite population spatial replicator.

The state of cell i at time index k of the cellular automaton is a tuple $\langle U_1(i, k), \dots, U_n(i, k) \rangle$ where $U_j(i, k)$ provides the size of the population of species j at position i at time k . For simplicity, we assume that species interaction may only happen between cells and not within cells; i.e., the $U_1(i, k)$ members of species 1 will not play against the $U_n(i, k)$ members of species n . This assumption will become irrelevant in the limit.

During state update, an agent A at cell i chooses a random direction (cell i') and a random member of the population (agent A') within that cell. Assume Agent A uses strategy r while Agent A' uses strategy s . After play, there are $\alpha \cdot \mathbf{A}_{rs}$ additional agents at cell i using strategy r and $\beta \cdot \mathbf{A}_{rs}$ additional agents playing strategy r at cell i' , where $\alpha + \beta = 1$ is the probability of motion from cell i to cell i' . If $\mathbf{A}_{rs} < 0$, then agents are removed from their respective cells. To avoid computational issues when more members of a species die than are present, \mathbf{A} can be modified so that $\mathbf{A}_{rs} \geq 0$ for all $r, s \in \{1, \dots, n\}$, without altering the evolutionary dynamics in proportion [2]. The update rule for a single agent is illustrated in Fig. 1. The process described above and illustrated in Fig. 1 is

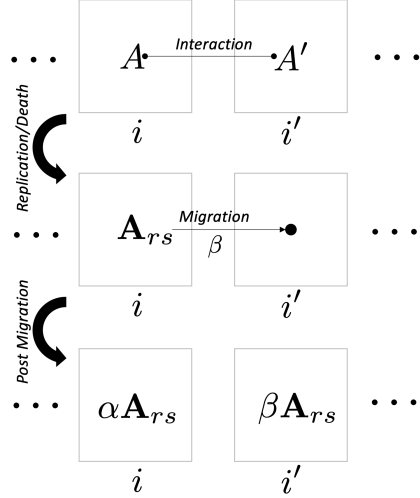


Figure 1: A single interaction between two agent in a spatial game on a one-dimensional lattice is illustrated. The direction of interaction is chosen at random. Motion is random and governed by α and β where $\alpha + \beta = 1$.

assumed to be happening simultaneously for each agent and we assume that the replication/death as a result of game play along with the migration are happening on (roughly) the same time scale. Using these assumptions, we can construct mean-field equations for the population U_r at position i and time $k + 1$ in a 1-D cellular automaton, assuming an equal likelihood that agents diffuse left or right. The mean number of agents playing strategy r present at position i at time $k + 1$ is determined by:

1. The expected number of agents who remain at cell i : $\alpha U_r(i, k)$
2. The expected number of new agents created at cell i who remain at cell i :

$$\frac{\alpha}{2} U_r(i, k) \left(\sum_s \mathbf{A}_{rs} (u_s(i + 1, k) + u_s(i - 1, k)) \right).$$

3. The expected number of agents who migrate to position i from neighboring cells:

$$\frac{\beta}{2} (U_r(i + 1, k) + U_r(i - 1, k)).$$

4. The expected number of agents created in a neighboring cell who migrate to cell i :

$$\frac{\beta}{2} (U_r(i + 1, k) + U_r(i - 1, k)) \sum_s \mathbf{A}_{rs} u_s(i, k).$$

Here $u_s(i, k)$ is the *proportion of the population* at cell i playing strategy s at time step k .

Let $\mathbf{u}(i, k) = \langle u_1(i, k), \dots, u_n(i, k) \rangle$. Re-writing sums as matrix products, the expected number of agents playing strategy r at cell i at time $k + 1$ is:

$$U_r(i, k + 1) = \alpha U_r(i, k) + \frac{\beta}{2} (U_r(i + 1, k) + U_r(i - 1, k)) + \frac{\alpha}{2} U_r(i, k) (\mathbf{e}_r^T \mathbf{A} (\mathbf{u}(i + 1, k) + \mathbf{u}(i - 1, k))) + \frac{\beta}{2} (U_r(i + 1, k) + U_r(i - 1, k)) \mathbf{e}_r^T \mathbf{A} \mathbf{u}(i, k). \quad (13)$$

Assume the cellular grid has lattice spacing Δx . Following [35] and using a Taylor approximation, we can write:

$$U_r(x, t + \Delta t) \approx U_r(x, t) + \Delta t \frac{\partial U_r(x, t)}{\partial t} + O(\Delta t^2)$$

$$U_r(x + \Delta x, t) \approx \sum_{j=0}^2 \frac{\Delta x^j}{j!} \frac{\partial^j U_r(x, t)}{\partial x^j} + O(\Delta x^3).$$

4 Derivation of Fluid Limits

We proceed to derive the mean-field approximation. Passing to the continuous case and assuming that interaction rates decrease linearly with Δt , we can write a second order approximation of Eq. (13) as:

$$\Delta t \frac{\partial U_r(x, t)}{\partial t} = \alpha U_r(x, t) + \beta \left(U_r(x, t) + \frac{1}{2} \Delta x^2 \frac{\partial^2 U_r}{\partial x^2} \right) + \alpha \Delta t U_r(x, t) \cdot \mathbf{e}_r^T \mathbf{A} \left(\mathbf{u}(x, t) + \frac{1}{2} \Delta x^2 \frac{\partial^2 \mathbf{u}}{\partial x^2} \right) + \beta \Delta t \left(U_r(x, t) + \frac{1}{2} \Delta x^2 \frac{\partial^2 U_r}{\partial x^2} \right) \mathbf{e}_r^T \mathbf{A} \mathbf{u}(x, t) - U_r(x, t). \quad (14)$$

Where the $-U_r(x, t)$ on the right-hand-side arises from the formation of the Newton quotient on the left-hand-side. Expanding and simplifying yields:

$$\Delta t \frac{\partial U_r(x, t)}{\partial t} = \frac{\beta}{2} \Delta x^2 \frac{\partial^2 U_r}{\partial x^2} + \Delta t U_r(x, t) \mathbf{e}_r^T \mathbf{A} \mathbf{u}(x, t) + \frac{\alpha \Delta t}{2} \Delta x^2 U_r(x, t) \mathbf{e}_r^T \mathbf{A} \frac{\partial^2 \mathbf{u}}{\partial x^2} + \frac{\beta \Delta t}{2} \Delta x^2 \frac{\partial^2 U_r}{\partial x^2} \mathbf{e}_r^T \mathbf{A} \mathbf{u}(x, t). \quad (15)$$

Assume $\beta \in (0, 1]$. Dividing through by Δt and assuming that $\lim_{\Delta t \rightarrow 0} \Delta x^2 / \Delta t = 2D / \beta$ yields:

$$\frac{\partial U_r(x, t)}{\partial t} = U_r(x, t) \mathbf{e}_r^T \mathbf{A} \mathbf{u}(x, t) + D \frac{\partial^2 U_r}{\partial x^2}. \quad (16)$$

The constant D is the diffusion constant and the assumption that

$$\lim_{\Delta t \rightarrow 0} \Delta x^2 / \Delta t = 2D / \beta$$

is a variant of the assumption used to derive Fick's Law [36] and identical when $\beta = 1$.

These are the spatial dynamics used by Durrett and Levin, (in the first part of their paper), but are derived only by adding a diffusion term to the standard finite population growth equations. In [19], Durrett and Levin note that they derive a set of equations they feel are more appropriate for modeling finite spatial systems. Their derivation at the end of [19] (for a specific hawk-dove system) rests on the assumption that migration happens “on a much faster timescale” than game interactions. Our model assumes that migration and game interactions occur on approximately the same time scale. Under this assumption, Eq. (16) is the correct spatial adaptation for finite populations; i.e., one simply adds a diffusion term. In the case where migration happens more quickly, then the derivation in [19] should be used instead.

5 Spatial Replicator with Finite Population

The derivation of Eqs. (1) and (2) are not given in [19]. They can be generalized for an arbitrary evolutionary game using Eq. (16) as the starting point. Let:

$$M(x, t) = \sum_s U_s(x, t).$$

Differentiating we have:

$$\frac{\partial U_r(x, t)}{\partial t M(x, t)} = \frac{1}{M(x, t)} \frac{\partial U_r(x, t)}{\partial t} - u_r(x, t) \sum_s \frac{1}{M(x, t)} \frac{\partial U_s(x, t)}{\partial t}.$$

Substituting from Eq. (16) we obtain:

$$\frac{\partial u_r}{\partial t} = u_r \cdot (\mathbf{e}_r^T \mathbf{A} \mathbf{u} - \mathbf{u}^T \mathbf{A} \mathbf{u}) + \frac{D}{M} \left(\frac{\partial^2 U_r}{\partial x^2} - u_r \cdot \sum_s \frac{\partial^2 U_s}{\partial x^2} \right). \quad (17)$$

Unlike in the derivation of the standard replicator dynamic, the rate of change of the population proportion is not solely a function of the proportions themselves.

We can remove dependence on the individual populations to derive an independent (coupled) system of differential equations that includes only the total population. For arbitrary strategy r , we can apply the quotient rule to obtain:

$$M \frac{\partial u_r}{\partial x} = \frac{\partial U_r}{\partial x} - u_r \frac{\partial M}{\partial x}$$

Differentiating again, multiplying by $1/M$ and re-arranging yields the expression:

$$\frac{1}{M} \frac{\partial^2 U_r}{\partial x^2} = \frac{u_r}{M} \frac{\partial^2 M}{\partial x^2} + \frac{2}{M} \frac{\partial u_r}{\partial x} \frac{\partial M}{\partial x} + \frac{\partial^2 u_r}{\partial x^2}.$$

Using this we can write

$$\frac{D}{M} \left(\frac{\partial^2 U_r}{\partial x^2} - u_r \sum_s \frac{\partial^2 U_s}{\partial x^2} \right) = D \left(\frac{2}{M} \frac{\partial M}{\partial x} \frac{\partial u_r}{\partial x} + \frac{\partial^2 u_r}{\partial x^2} \right)$$

Using this we can re-write Eq. (17) as:

$$\frac{\partial u_r}{\partial t} = u_r \cdot (\mathbf{e}_r^T \mathbf{A} \mathbf{u} - \mathbf{u}^T \mathbf{A} \mathbf{u}) + D \left(\frac{2}{M} \frac{\partial M}{\partial x} \frac{\partial u_r}{\partial x} + \frac{\partial^2 u_r}{\partial x^2} \right). \quad (18)$$

The dynamics of M can be derived (by addition) from Eq. (16):

$$\frac{\partial M}{\partial t} = M \mathbf{u}^T \mathbf{A} \mathbf{u} + D \frac{\partial^2 M}{\partial x^2}.$$

Thus, we have a coupled set of differential equations written entirely in terms of \mathbf{u} and M , rather than U_r , M and \mathbf{u} :

$$\forall r \begin{cases} \frac{\partial u_r}{\partial t} = u_r \cdot (\mathbf{e}_r^T \mathbf{A} \mathbf{u} - \mathbf{u}^T \mathbf{A} \mathbf{u}) + \\ D \left(\frac{2}{M} \frac{\partial M}{\partial x} \frac{\partial u_r}{\partial x} + \frac{\partial^2 u_r}{\partial x^2} \right) \\ \frac{\partial M}{\partial t} = M \mathbf{u}^T \mathbf{A} \mathbf{u} + D \frac{\partial^2 M}{\partial x^2} \end{cases}. \quad (19)$$

This is the spatial replicator equation for *finite* populations. Letting $M = s$ and $D = 1$, we recover the dynamics of Durrett and Levin. In contrast to the aspatial replicator, the inclusion of dynamics for M yields a linearly independent system of differential equations.

Allowing M to approach infinity uniformly in x , we arrive at the fluid limit in terms of \mathbf{u} alone; this is the 1D nonlinear reaction-diffusion equation used by Vicker's [16, 17]:

$$\forall r \left\{ \frac{\partial u_r}{\partial t} = u_r \cdot (\mathbf{e}_r^T \mathbf{A} \mathbf{u} - \mathbf{u}^T \mathbf{A} \mathbf{u}) + D \frac{\partial^2 u_r}{\partial x^2} \right. . \quad (20)$$

Generalization to N -dimensions is straightforward by replacing ∂_x^2 with the Laplacian Δ . The N -dimensional spatial replicator with finite population is given by:

$$\forall r \begin{cases} \frac{\partial u_r}{\partial t} = u_r \cdot (\mathbf{e}_r^T \mathbf{A} \mathbf{u} - \mathbf{u}^T \mathbf{A} \mathbf{u}) + D \left(\frac{2}{M} \nabla M \cdot \nabla u_r + \Delta u_r \right) \\ \frac{\partial M}{\partial t} = M \mathbf{u}^T \mathbf{A} \mathbf{u} + D \Delta M. \end{cases}$$

Thus, the finite population case adds a nonlinear convection term that forces u_r to follow the population gradient. A similar system is studied by deForest and Belmonte in [11], where the payoff gradient is followed instead of the population gradient.

In both Eqs. (19) and (20), we see that the aspatial replicator dynamics appear on the right hand side perturbed by a spatial term. It is well known that the dynamics of the aspatial replicator are confined to the n -dimensional simplex Δ_n . This remains true for the spatial replicator dynamics with finite populations. Moreover, the solution $u_r = 1$ (i.e., there is only one population) is a fixed point for the spatial replicator dynamic since the spatial derivative of the probability distribution of the population proportions is zero and the time derivative is identically zero as expected. Thus, pure populations are constant stationary solutions for these dynamics. Lastly, if $\tilde{\mathbf{u}}(x, t)$ is a constant solution at a Nash equilibrium for the game defined by \mathbf{A} , then the right-hand-side is again identically zero by the Folk Theorem [4] of evolutionary game theory together with the fact that there is no spatial variation. Thus every Nash equilibrium of the matrix game corresponds to a spatially constant stationary solution of the spatial replicator dynamic in both the finite and infinite population cases.

6 One Dimensional Rock-Paper-Scissors

Durrett and Levin's analysis of Hawk-Dove was aided by the fact that one strategy can be eliminated, leaving a coupled system of two partial differential equations. In the remainder of this paper,

we analyze variations of rock-paper-scissors (RPS), which yield more interesting results because of its cyclic three-strategy nature and because it can be easily parameterized as discussed in [2]. We note again, substantial work has been done on spatial RPS [20–23, 25–28] with a major focus on identifying spatial structures (e.g., spirals) that can emerge from these dynamics. We note a portion of the work in these references is focused on analyze the Hopf bifurcation that occurs in their RPS dynamics. This is not needed when we begin with the replicator since Zeeman’s work [30] discusses RPS as a degenerate Hopf bifurcation and completely characterizes the phase space for all possible parameters. Therefore, the objective in the remainder of this work is to compare the finite and infinite population replicator for a more interesting three strategy game. We will also investigate the discrete time / discrete space model and compare these to the continuous variants. Finally, for simplicity (and in contrast to much of the previous work in spatial RPS), we focus our attention on the one-dimensional PDE. Finally we note that unlike the results in (e.g. [20, 23, 27]) we do not expect to illustrate spirals or more complex phenomena because we focus on the one-dimensional case as did Durrett and Levin [19].

A generalized RPS payoff matrix is given by:

$$\mathbf{A} = \begin{bmatrix} 0 & -1 & 1+a \\ 1+a & 0 & -1 \\ -1 & 1+a & 0 \end{bmatrix}.$$

When $a = 0$, this is the standard RPS game which has Nash equilibrium $\langle \frac{1}{3}, \frac{1}{3}, \frac{1}{3} \rangle$. This is the unique interior fixed point and the aspatial replicator exhibits an elliptic fixed point at this Nash equilibrium. This Nash equilibrium is preserved for $a \neq 0$; and corresponds to an asymptotically stable interior fixed point when $a > 0$ and unstable fixed point when $a < 0$ [30].

Let $\mathbf{u} = \langle u_r, u_p, u_s \rangle$ and note:

$$\zeta(u_r, u_p, u_s) \triangleq \mathbf{u}^T \mathbf{A} \mathbf{u} = a(u_r u_s + u_r u_p + u_s u_p).$$

There are at least two classes of global solutions to Eq. (19):

Stationary Solution Here, $u_r = u_p = u_s = \frac{1}{3}$ and M solves:

$$0 = \frac{a}{3}M + M''$$

or there is a single population (e.g., $u_r = 1$) and M is constant in x .

Oscillating Solution Here, $u_*(x, t) \equiv v_*(t)$ with $*$ $\in \{r, p, s\}$ where v_r, v_p, v_s are solutions to the standard RPS replicator and $M(x, t) = \mu(t)$ satisfies linear equation:

$$\dot{\mu} = \zeta(v_r, v_p, v_s)\mu.$$

Solutions of this kind are also present for Eq. (20). The stationary solution class is relevant to our analysis of the $a > 0$ case. The oscillating solution captures the long-run behavior of $a = 0$ case under finite population dynamics in continuous time. We consider the $a < 0$ case more deeply in the sequel.

6.1 The case when $a = 0$

When $a = 0$, we have $\zeta(u_r, u_s, u_p) = 0$ so that M is governed by the heat equation with diffusion constant D . Assuming appropriate initial and boundary conditions, there is a global solution,

$M(x, t)$. We express the convection coefficient of $\partial_x u_*$ in Eq. (19) in terms of this solution:

$$\epsilon(x, t) = \frac{2D\partial_x M(x, t)}{M(x, t)}.$$

Under appropriate boundary conditions, diffusion of the (locally) finite population implies that:

$$\begin{aligned} \lim_{t \rightarrow \infty} M(x, t) &= M^* > 0 \\ \lim_{t \rightarrow \infty} \epsilon(x, t) &= 0. \end{aligned}$$

Therefore, asymptotically (in time), any solution of Eq. (19) must also satisfy Eq. (20). Interestingly, the convection term in the finite population case can drive the long-term behavior of the system to the oscillating solution while the infinite population spatial replicator equation converges to the stationary solution. To see this, let $a = 0$, $D = 1$ and assume a periodic boundary condition (evolution on an annulus or S^1) with $M(-\pi, t) = M(\pi, t)$, $u_*(-\pi, t) = u_*(\pi, t)$ ($* \in \{r, p, s\}$). Assume:

$$M(x, 0) = 2 + \cos(x) \tag{21}$$

so that:

$$\begin{aligned} M(x, t) &= 2 + e^{-t} \cos(x) \\ \epsilon(x, t) &= \frac{-2e^{-t} \sin(x)}{2 + e^{-t} \cos(x)}. \end{aligned}$$

Assuming:

$$u_r(x, 0) = \frac{1}{3}(1 + \sin(x - 4\pi/3)) \tag{22}$$

$$u_p(x, 0) = \frac{1}{3}(1 + \sin(x - 2\pi/3)) \tag{23}$$

$$u_s(x, 0) = \frac{1}{3}(1 + \sin(x)). \tag{24}$$

Unless otherwise noted, these are the initial conditions for all numerical examples. The (numerically computed) solution to Eq. (19) is illustrated in Fig. 2. Notice the long-run behavior is consistent with the oscillating solution. Since $\zeta(v_r, v_p, v_s) \equiv 0$ and we assumed a periodic boundary condition, M must approach a trivial stationary solution; i.e., $M(x, \infty) = 2$. By way of comparison a (numerical) solution to the infinite population spatial replicator equation is shown in Fig. 3. In this case, the long-run behavior is consistent with the stationary solution. In the aspatial replicator the fixed point corresponding to the Nash equilibrium is neutrally stable. Thus, the fixed point is stabilized by the diffusion terms in Eq. (20).

We compare this to the finite population case in discrete time in Section 8 below.

6.2 The case when $a > 0$

When $a > 0$, the stationary solution for M must satisfy:

$$M(x) = C_1 \sin\left(\sqrt{\frac{a}{3}}x\right) + C_2 \cos\left(\sqrt{\frac{a}{3}}x\right).$$

However, this solution is non-physical because it admits negative population counts and it is clear from Eq. (19) that for nonnegative initial conditions, solutions will remain nonnegative. Therefore, when $a > 0$, the finite population spatial replicator will not admit a stationary solution. Instead we find that $M(x, t) \rightarrow \infty$ and $t \rightarrow \infty$ so that solutions asymptotically satisfy Eq. (20).

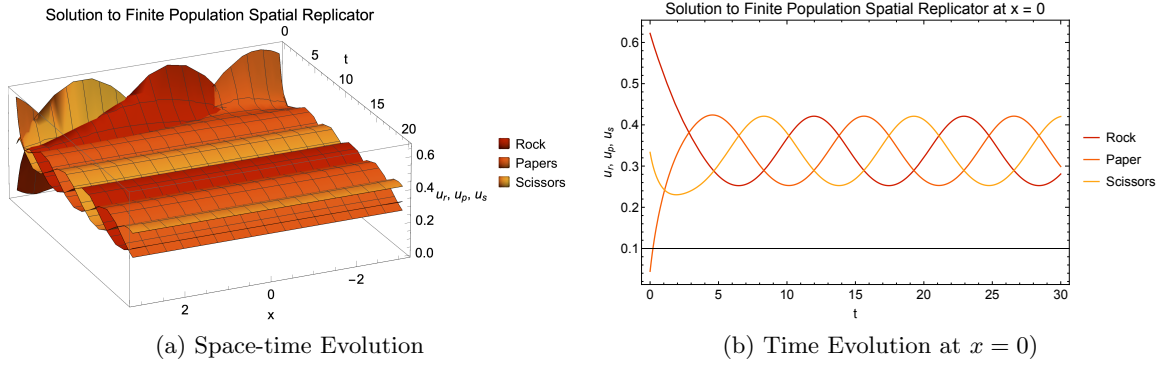


Figure 2: Evolution of the finite population spatial replicator converges to an oscillating solution when $a = 0$. (a) The population proportions at various points in space and time are shown. (b) A slice of the population is shown at $x = 0$.

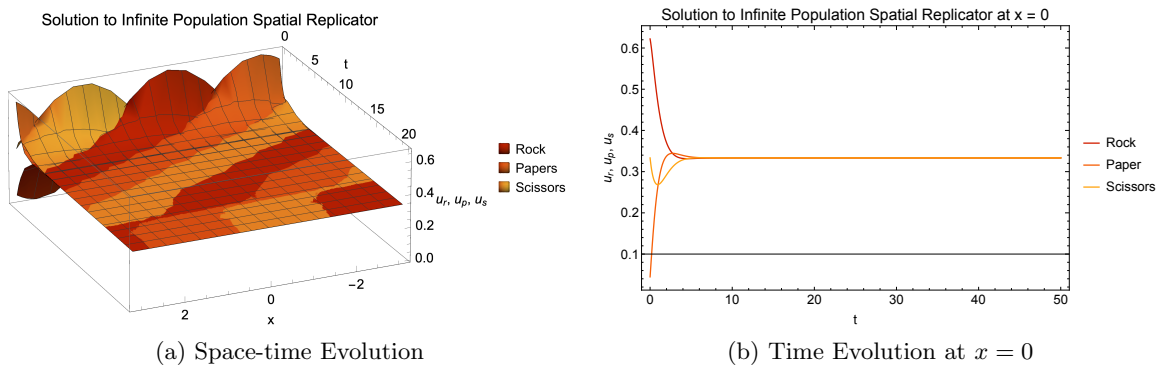


Figure 3: Evolution of the infinite population spatial replicator converges to a steady state solution when $a = 0$. This is surprising since the Nash equilibrium fixed point is neutrally stable in the aspatial replicator [30]. (a) The population proportions at various points in space and time are shown. (b) A slice of the population is shown at $x = 0$.

To see this we combine the fact that $\langle \frac{1}{3}, \frac{1}{3}, \frac{1}{3} \rangle$ is an asymptotically stable fixed point of the aspatial replicator with a maximum principle argument for $\frac{\partial u_r}{\partial t}$ in Eq. (19) and note that for any initial condition in the interior of Δ_3 there is some $\zeta_0 > 0$ so that $\zeta(u_r, u_p, u_s) \geq \zeta_0$. It follows that the solution $M(x, t)$ is bounded below by the solution of

$$\dot{m}(t) = \zeta_0 m, \quad m(0) = \min_x M(x, 0) \quad (25)$$

In particular, M is increasing everywhere and $M(x, t) \rightarrow \infty$ as $n \rightarrow \infty$. Consequently, $\epsilon(x, t) \rightarrow 0$ for large t and any solution to Eq. (19) must asymptotically satisfy Eq. (20). This is illustrated in Fig. 4 (here $D = \frac{1}{2}$, $a = \frac{1}{10}$). Furthermore, linear stability analysis of Eq. (20) suggests that

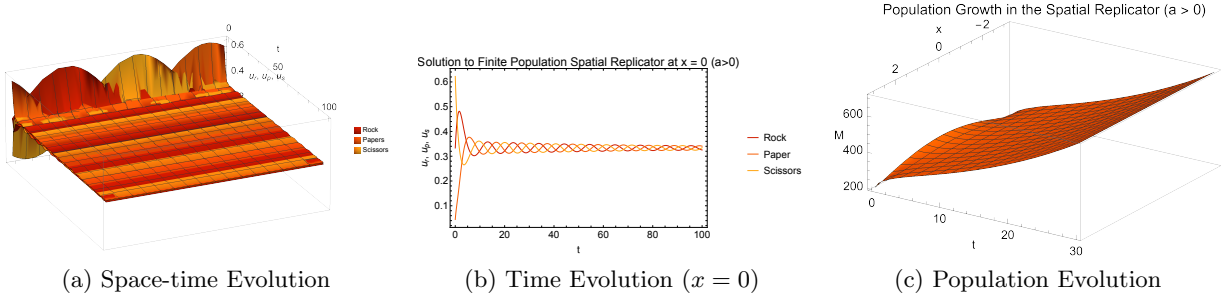


Figure 4: The evolution of the finite population spatial replicator is shown for $a > 0$. The population proportions u_r, u_p, u_s quickly approach the oscillating solution. As M increases, these oscillations decay and the population proportions approach the stationary solution of the infinite population case. (a) The population is shown at various points in space-time. (b) A slice of the population is shown evolving. (c). The cumulative population function is shown increasing over all space and time.

the steady state solution $u_r = u_p = u_s = \frac{1}{3}$ should be asymptotically stable for Eq. (20) (see Theorem 1 of [37]), since the aspatial replicator dynamics with $a > 0$ has an asymptotically stable fixed point at the Nash equilibrium (see [30] or [4]). Our simulation suggests dynamics on two time scales. Solutions quickly approach an oscillating solution. The oscillations in population proportions u_r, u_p, u_s then slowly decay toward the fixed point of the aspatial replicator as M increases. When $a < 0$, the dynamics are more interesting, as we demonstrate below.

7 Traveling Waves When $a < 0$

Consider the infinite population model first. Letting $z = x - ct$, we can re-write Eq. (20) in compact form as:

$$\forall i \begin{cases} Dv'_i = -u_i (\mathbf{e}_i^T \mathbf{A} \mathbf{u} - \mathbf{u}^T \mathbf{A} \mathbf{u}) - cv_i \\ u'_i = v_i \end{cases} \quad (26)$$

For RPS we have the six dimensional linear system:

$$\begin{aligned}
Dv'_r &= au_r\zeta(u_r, u_s, u_p) - u_r(u_s - u_p) - au_ru_s - cv_r \\
u'_r &= v_r \\
Dv'_p &= au_p\zeta(u_r, u_s, u_p) - u_p(u_r - u_s) - au_pu_r - cv_p \\
u'_p &= v_p \\
Dv'_s &= au_s\zeta(u_r, u_s, u_p) - u_s(u_p - u_r) - au_su_p - cv_s \\
u'_s &= v_s.
\end{aligned}$$

These equations are structurally similar to those found in [20] and the analysis proceeds in a similar way, with different specific computations for the system we consider. If \mathbf{u}^* is a Nash equilibrium of \mathbf{A} , then the pair $\mathbf{u} = \mathbf{u}^*$ and $\mathbf{v} = \mathbf{0}$ is a fixed point of Eq. (26). Linearizing about $u_r = u_p = u_s = \frac{1}{3}$, $v_r = v_p = v_s = 0$, we obtain the eigenvalues:

$$\begin{aligned}
\lambda_{1,2} &= \frac{-3c \pm \sqrt{9c^2 + 12aD}}{6D} \\
\lambda_{3,4} &= \frac{-3c \pm \sqrt{9c^2 + 6aD + 6D\sqrt{3}\sqrt{-(a+2)^2}}}{6D} \\
\lambda_{5,6} &= \frac{-3c \pm \sqrt{9c^2 + 6aD - 6D\sqrt{3}\sqrt{-(a+2)^2}}}{6D}.
\end{aligned}$$

We can simultaneously show that for appropriate choice of wave speed, a center manifold exists and therefore a non-decaying traveling wave solution exists for the PDE. As a by-product, we compute the wave speed for a non-decaying traveling wave in terms of a and D . Assume $a \in (-2, 0)$. For some constant b (to be determined), let:

$$(3c \pm bi)^2 = 9c^2 + 6aD \pm 6D\sqrt{3}\sqrt{-(a+2)^2} = 9c^2 + i6aD \pm 6D(a+2)\sqrt{3}.$$

Expanding the left hand side and relating real and imaginary parts we have:

$$\begin{aligned}
9c^2 - b^2 &= 9c^2 + 6aD \\
6bc &= 6D(a+2)\sqrt{3}.
\end{aligned}$$

Solving for b and c yields:

$$\begin{aligned}
b &= \sqrt{-6aD} \\
\pm \tilde{c} &= \pm \frac{(a+2)\sqrt{2k}}{2\sqrt{-a}}
\end{aligned}$$

Without loss of generality, assume positive \tilde{c} . Using this information, we can obtain:

$$\begin{aligned}
\tilde{\lambda}_{1,2} &= \frac{-3\tilde{c} \pm \sqrt{9\tilde{c}^2 + 12aD}}{6D} \\
\tilde{\lambda}_3 &= \frac{-6\tilde{c} - bi}{6D} \\
\tilde{\lambda}_4 &= \frac{bi}{6D} \\
\tilde{\lambda}_5 &= \frac{-6\tilde{c} + bi}{6D} \\
\tilde{\lambda}_6 &= \frac{-bi}{6D}.
\end{aligned}$$

Our assumption that $a < 0$ and the fact that $\tilde{c} > 0$ implies that $\text{Re}(\lambda_{1,2}) < 0$ for all choices of $D > 0$ and $a \in (-2, 0)$. Therefore, this system has a four dimensional stable manifold and the existence of two pure imaginary eigenvalues suggests a center manifold that allows the emergence of the traveling wave solution.

Naturally, if $c \neq \tilde{c}$, there may still be a traveling wave, but its amplitude will decay ($c > \tilde{c}$) or grow in time ($c < \tilde{c}$). Starting from the PDE it is difficult to determine what wave speed will emerge (and therefore its relationship to a and D) given the initial conditions. However, traveling waves can be observed with both increasing and decreasing amplitude; fine tuning the parameters leads to a numerically stable traveling wave over the region of integration. This is illustrated in the PDE system in Fig. 5 using $a = -0.79$ and $D = \frac{1}{12}$. For completeness, we note the negative wave

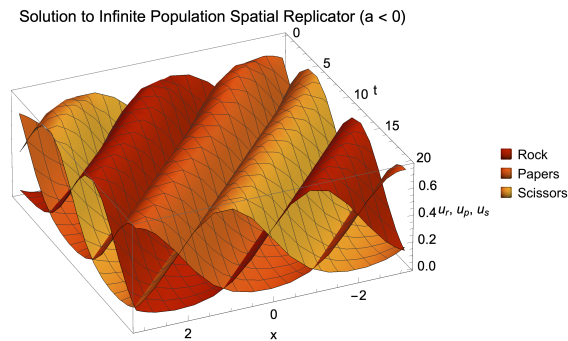


Figure 5: An example of a stable amplitude traveling wave solution is illustrated for RPS when $a < 0$. For this example $a = -0.79$ and $D = 1/12$. The plot shows the population evolution over space and time.

speed solution $-\tilde{c}$ implies an unstable fixed point (consistent with $a < 0$ in the aspatial replicator dynamic). In this case, we would expect to see the proportions oscillate with increasing amplitude.

When the population is finite and $a < 0$, there is a value $\zeta_0 > 0$ so that $\zeta(u_r, u_p, u_s) \leq -\zeta_0$ on the interior of Δ_3 . It follows from Eq. (25) (substituting $-\zeta_0$ for ζ_0) that the population on the real line (or an annulus) will collapse. As $M(x, t) \rightarrow 0$ everywhere, numeric solutions of the equation can become unstable. Interestingly, the finite population term seems to impact the symmetry of the wave fronts in the traveling wave that was illustrated in Fig. 5. This effect is illustrated in Fig. 6 in which we illustrate a top-down side-by-side comparison of the waves generated by both the infinite population replicator and the finite population replicator with $a = -0.79$ and $D = \frac{1}{12}$. The finite (collapsing) population seems to cause the variations in the wave front boundaries. Additionally, the wave seen in Figure 6b is not stable. The amplitudes of u_r, u_s, u_t are increasing in time (see Fig. 7 This is most likely due to the fact that the finite population (convection) term is acting like additional diffusion as the population collapse.

8 Comparison to Discrete Space and Time Models

We compare a subset of the results presented thus far to the discrete space/time model described in Section 3. For brevity, we focus on the case when $a = 0$ or $a < 0$. We used 300 grid points arranged on a ring. Each grid point had a population of rock, paper and scissors defined at it. One hundred replications of the stochastic dynamics illustrated in Fig. 1 were performed and the results averaged together to construct an approximated mean field dynamic. We constructed a discrete version of the initial conditions given in Eqs. (22) to (24) and the total initial population Eq. (21). In order to manage population collapse (especially when $a < 0$), we multiplied the total

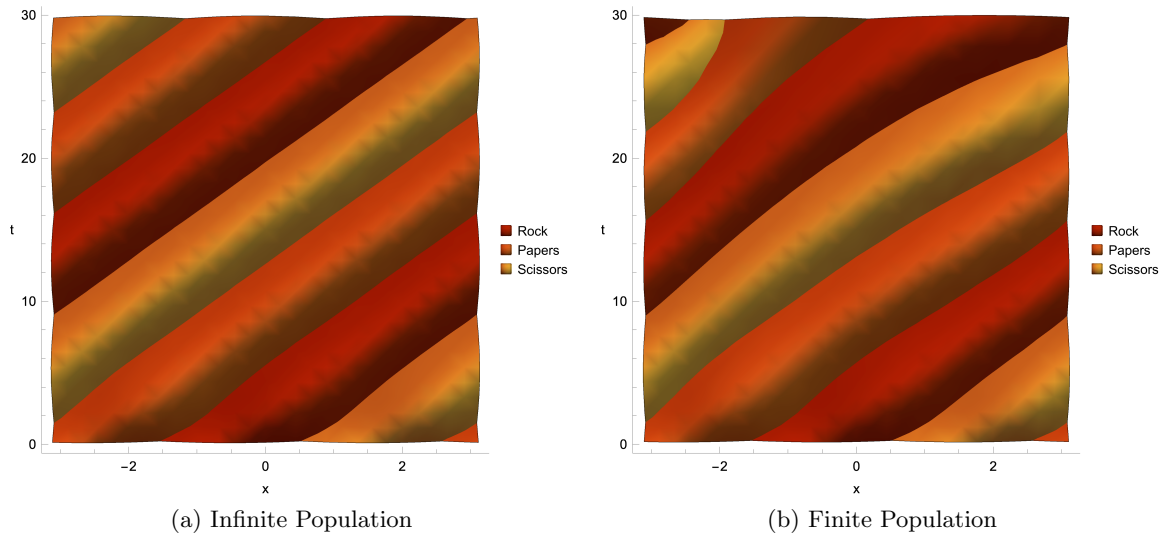


Figure 6: We compare the dynamics of a stable traveling wave (top) and the resulting unstable wave that results when finite populations are considered (bottom). An overhead viewpoint is used to illustrate asymmetry in the wave fronts in the finite population case.

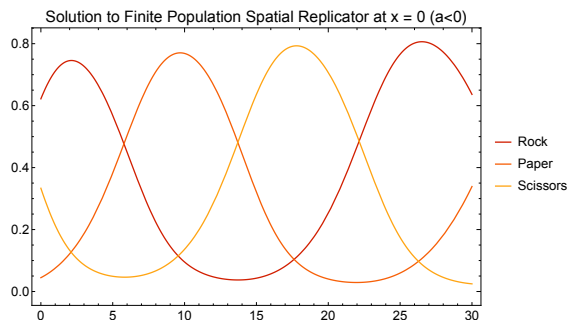


Figure 7: The amplitude of the traveling wave increases in the finite population case (shown at $x = 0$). This is consistent with the asymptotically unstable nature of the equilibrium when $a < 0$ [30].

population by a factor of 20 for $a = 0$ and 75 when $a < 0$. Population distributions over time are shown in Fig. 8. Each simulation was terminated when any cell experienced population collapse (as the update dynamics are not defined beyond that point). The mean behavior was computed using data from each simulation prior to any population collapse.

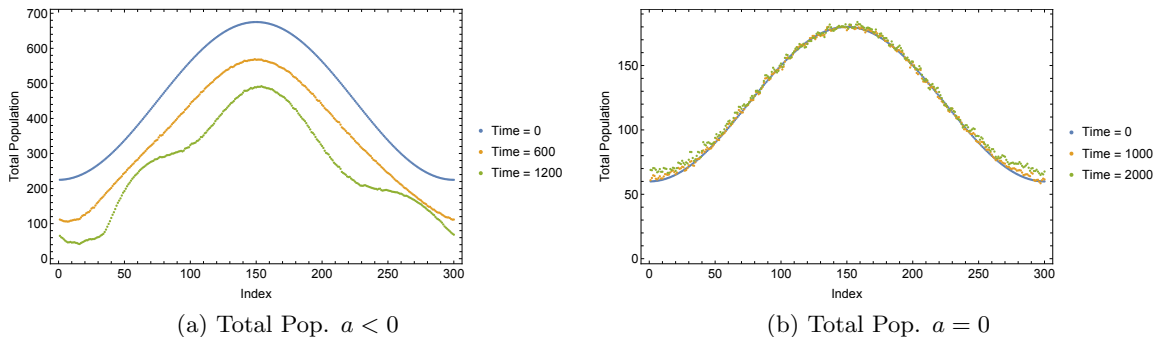


Figure 8: We show the mean population distributions over time for the discrete model (100 runs) described in Section 3 for the cases (top) $a < 0$ and (bottom) $a = 0$. Notice the population is collapsing when $a < 0$, while it is relatively stable over long periods of time for the case when $a = 0$. This is to be expected since the mean population increase and decrease is equal to zero.

For the case when $a < 0$, the mean field dynamics are illustrated in Fig. 9a. As in Fig. 6b, we see a traveling wave with variations in the wave fronts. Due to population collapse (illustrated in Fig. 8-top), there is not as much behavioral variation in the discrete space/time cellular automaton model as there is in the finite population replicator dynamic. This is due to the fact that population collapse happens before any novel features can emerge. Inspection of wave fronts, however, shows the same irregularities as in solutions to the finite population partial differential equation. The population proportions at the point $x = 150$ is shown in Fig. 9b. The population proportion amplitudes may be increasing, but it is difficult to determine from this plot because of simulation termination at population collapse.

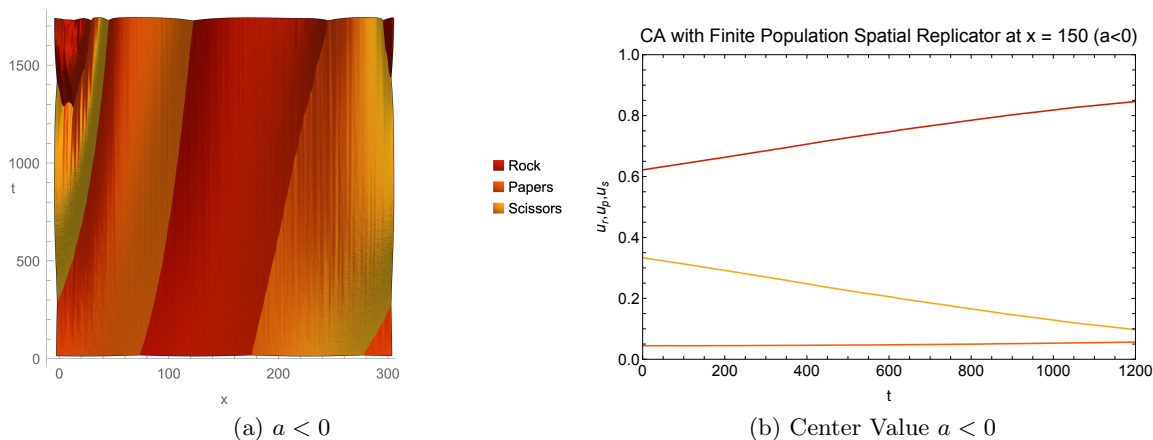


Figure 9: We illustrate the mean dynamics of the discrete space/time RPS game with $a < 0$ taken over 100 runs. As in the case with the finite spatial replicator. The wave fronts (seen overhead) also exhibit similar characteristics to those in Fig. 6b. The population proportion amplitudes may be increasing, but it is difficult to determine from this plot.

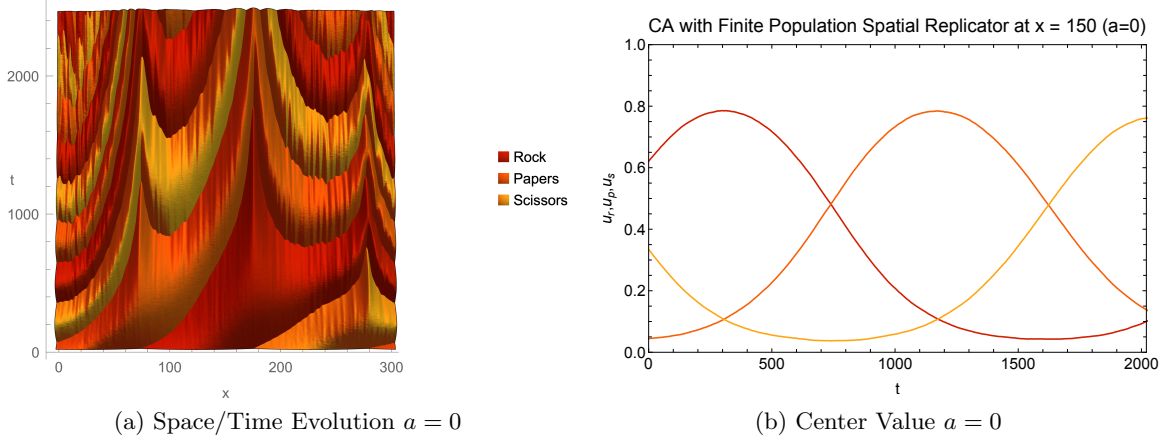


Figure 10: We illustrate the mean dynamics of the discrete space/time RPS game with $a = 0$ taken over 100 runs. We note that the population at the center point seems to be converging to the stationary solution, in contrast to the finite spatial replicator example. This may be because of the size of the initial populations chosen.

We contrast this with the discrete space/time model when $a = 0$. The mean field dynamics are shown in Figs. 10a and 10b. The dynamics show much more variation than those in Fig. 2 or Fig. 3. However it is clear that no clear traveling wave is forming. The amplitude decrease in the population proportion at $x = 150$ (Fig. 10b) is extremely slight when compared to Fig. 3. As expected the population is not collapsing in the case when $a = 0$ since, on average, we should see only diffusion of the total population rather than death or birth.

9 Stable Steady State with $a < 0$

If the population size is held constant at the boundary (i.e., we replace the periodic boundary conditions with Dirichlet boundary conditions) then steady state analysis becomes possible in the finite population. Consider the steady state solution $u_r = u_p = u_s = \frac{1}{3}$. The population steady state equation is:

$$0 = -\frac{a}{3}M + D\frac{\partial^2 M}{\partial x^2}.$$

Imposing the non-zero symmetric boundary conditions $M(-L, t) = M(L, t) = m_0 > 0$ yields the steady state solution:

$$M(x) = \alpha \cosh\left(\frac{\sqrt{-a}}{\sqrt{3D}}x\right),$$

where:

$$\alpha = m_0 \operatorname{sech}\left(\frac{\sqrt{-a}}{\sqrt{3D}}L\right).$$

Unlike the steady state solution for M when $a > 0$, this is physically realizable. When $L = \pi$ and we operate on an annulus, we may imagine a point (at $x = \pm\pi$) where population is held constant and then moves around the annulus to die. Suppose that $u_*(L, t) = u_*(-L, t) = \frac{1}{3}$ ($* \in \{r, p, s\}$). We *conjecture* that the steady state solution is stable for the finite population replicator. This is

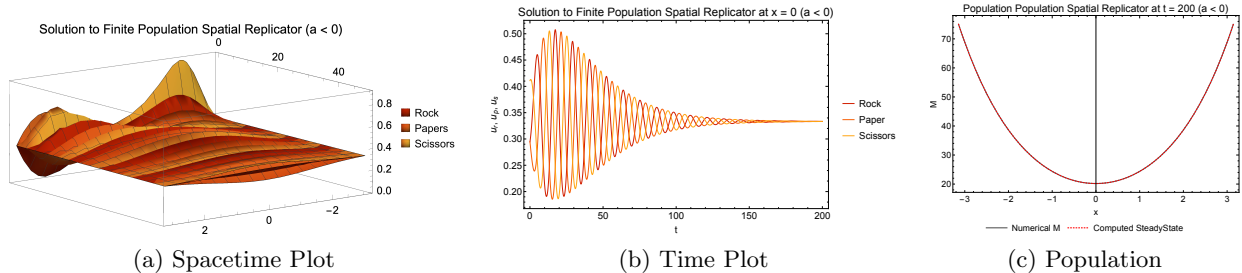


Figure 11: A stable stationary solution is illustrated with a “valley of death” for the population. (a) a space/time plot show the population overall converging to the stationary distribution. This is reinforced in (b), which illustrates this for $x = 0$ over all time. The total population is shown in (c) and shows the “valley of death” caused by the Dirichlet boundary conditions.

illustrated in Fig. 11 using the modified initial condition:

$$\begin{aligned}
 u_r(x, 0) &= \frac{f_r(x)}{f_r(x) + f_p(x) + f_s(x)} \\
 u_p(x, 0) &= \frac{f_p(x)}{f_r(x) + f_p(x) + f_s(x)} \\
 u_s(x, 0) &= \frac{f_s(x)}{f_r(x) + f_p(x) + f_s(x)} \\
 M(x, 0) &= f_r(x) + f_p(x) + f_s(x),
 \end{aligned}$$

with

$$\begin{aligned}
 f_r(x) &= 25 + x^2(x - \pi)(x + \pi) \\
 f_p(x) &= 25 - 2x(x - \pi)(x + \pi) \\
 f_s(x) &= 25 - (x - \pi)(x + \pi).
 \end{aligned}$$

These equations satisfies the Dirichlet boundary condition $u_*(-\pi) = u_*(\pi) = \frac{1}{3}$ and $M(-\pi) = M(\pi) = 75$. (The exact value of m_0 is irrelevant.) In Fig. 11, we set $a = -\frac{1}{10}$ and $D = \frac{1}{12}$. The long-run behavior of $M(x, t)$ is shown in Fig. 11c. It is clear that the solution has converged to the stationary state.

It is worth nothing that the stability of the steady state solution is entirely a function of the Dirichlet boundary conditions. To see this, we can use use the initial population distributions from Eqs. (22) to (24) with consistent boundary conditions. In this case, a standing wave emerges in the finite population spatial replicator as the long-run behavior and the long-run population behavior is no longer described by a hyperbolic cosine. This is shown in Fig. 12a. By way of comparison, the corresponding Dirichlet boundary conditions in infinite population spatial replicator equation yield a highly complex wave structure that is similar to the oscillating solutions identified earlier (see Fig. 12b).

10 Conclusion

In this paper we studied a finite and infinite population spatial replicator. We showed how the finite population spatial replicator can be derived from first principles from a stochastic cellular

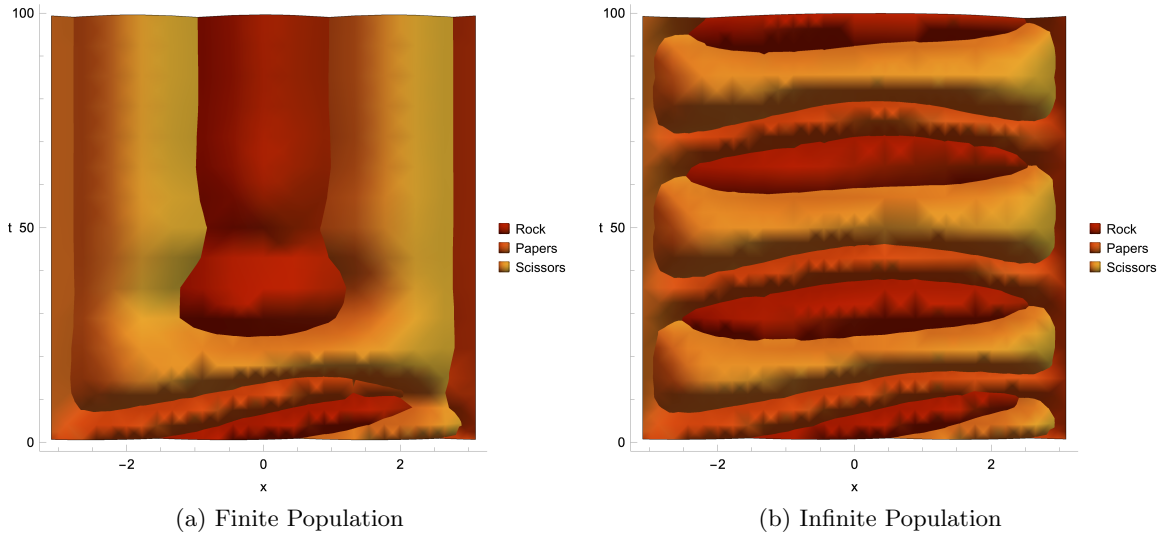


Figure 12: A comparison of the finite and infinite population replicator with Dirichlet boundary conditions and $a < 0$ illustrates a standing wave in the finite population case and an oscillating pattern in the infinite population case.

automaton model and from there how the infinite population replicator used by Vickers [16, 17] follows from this. This result generalizes the work of Durrett and Levin [19] who first derived and studied the finite population spatial replicator for a specific game. We then compared the finite and infinite population spatial replicator for rock-paper-scissors on a one dimensional annulus one dimension (S^1). Our results are consistent with the work in [20–23, 25–28], which studies various characteristics of RPS, not necessarily in connection with spatial replicator. Consistent with the work in [20, 27] we show that for a certain rock-paper-scissors variant stable amplitude traveling waves can emerge as solutions to the infinite population spatial replicator, but these are destroyed by population collapse in the finite population spatial replicator. We studied population collapse using Dirichlet boundary conditions on S^1 and illustrated the structure of steady state solutions, including standing waves.

The finite population spatial replicator is intriguing because it is a highly non-linear reaction-convection-diffusion equation where convection is governed by the per capita bulk population motion. Consequently, it may be particularly useful for studying human behavior, where large populations tend to move as a result of regional crises and strategies (i.e., behaviors) may represent human interaction patterns. Studying a simpler game (as Durrett and Levin did with Hawk-Dove) may illustrate additional behaviors. Certainly proving our conjecture that when $u_*(L, t) = u_*(-L, t) = \frac{1}{3}$ ($* \in \{r, p, s\}$) and $M(L, t) = M(-L, t) = m_0$ the finite population spatial replicator converges to the proposed steady state solution is a clear future direction. In addition to this, identifying more ways in which the finite and infinite spatial replicators differ in terms of solutions would be interesting. The most interesting differences in the case of RPS seem to occur when the population is collapsing. It would be intriguing to find cases where population collapse is not the main driver in behavioral differences, since tautologically this must cause differences in finite vs. infinite population equations. Additionally, further comparison to the work in [20–23, 25–28] may show additional dynamics (e.g., spirals) that can emerge in the two-dimensional version of the finite population spatial replicator.

Acknowledgement

Portions of CG's work were supported by the National Science Foundation Grant CMMI-1932991.

References

- [1] D. Friedman. Evolutionary games in economics. *Econometrica*, 59:637–666, 1991.
- [2] J. W. Weibull. *Evolutionary Game Theory*. MIT Press, 1997.
- [3] J. Hofbauer and K. Sigmund. *Evolutionary Games and Population Dynamics*. Cambridge University Press, 1998.
- [4] J. Hofbauer and K. Sigmund. Evolutionary Game Dynamics. *Bulletin of the American Mathematical Society*, 40(4):479–519, 2003.
- [5] Daniele Vilone, Alberto Robledo, and Angel Sánchez. Chaos and unpredictability in evolutionary dynamics in discrete time. *Phys. Rev. Lett.*, 107:038101, Jul 2011.
- [6] Andrew J. Black, Arne Traulsen, and Tobias Galla. Mixing times in evolutionary game dynamics. *Phys. Rev. Lett.*, 109:028101, Jul 2012.
- [7] Danielle F. P. Toupo and Steven H. Strogatz. Nonlinear dynamics of the rock-paper-scissors game with mutations. *Phys. Rev. E*, 91(052907), 2015.
- [8] K. H. Schlag. Why imitate and if so how? A boundedly rational approach to multi-armed bandits. *J. Econ. Theory*, 78:130–156, 1997.
- [9] D. Fudenberg and D. K. Levine. *The theory of learning in games*. MIT Press, 1998.
- [10] G. Bard Ermentrout, Christopher Griffin, and Andrew Belmonte. Transition matrix model for evolutionary game dynamics. *Phys. Rev. E*, 93:032138, Mar 2016.
- [11] R deForest and A Belmonte. Spatial pattern dynamics due to the fitness gradient flux in evolutionary games. *Physical Review E*, 87, 2013.
- [12] B Kerr, MA Riley, MW Feldman, and Bohannan BJM. Local dispersal promotes biodiversity in a real-life game of rock–paper–scissors. *Nature*, 418.6894:171–174, 2002.
- [13] MA Nowak and RM May. Evolutionary games and spatial chaos. *Nature*, 359.6398:826–829, 1992.
- [14] CP Roca, JA Cuesta, and A Sánchez. Evolutionary game theory: Temporal and spatial effects beyond replicator dynamics. *Physics of life reviews*, 6.4:208–249, 2009.
- [15] G Szabó, A Szolnoki, and R Izsák. Rock-scissors-paper game on regular small-world networks. *Journal of physics A: Mathematical and General*, 37.7:2599, 2004.
- [16] GT Vickers. Spatial patterns and ess's. *Journal of Theoretical Biology*, 140(1):129–135, 1989.
- [17] GT Vickers. Spatial patterns and travelling waves in population genetics. *Journal of Theoretical Biology*, 150:329–337, 1991.

- [18] R Cressman and GT Vickers. Spatial and density effects in evolutionary game theory. *Journal of theoretical biology*, 184(4):359–369, 1997.
- [19] R. Durrett and S. Levin. The Importance of Being Discrete (and Spatial). *Theoretical Population Biology*, 46:363–394, 1994.
- [20] Claire M Postlethwaite and Alastair M Rucklidge. A trio of heteroclinic bifurcations arising from a model of spatially-extended rock–paper–scissors. *Nonlinearity*, 32(4):1375, 2019.
- [21] Bartosz Szczesny, Mauro Mobilia, and Alastair M Rucklidge. Characterization of spiraling patterns in spatial rock-paper-scissors games. *Physical Review E*, 90(3):032704, 2014.
- [22] Attila Szolnoki, Mauro Mobilia, Luo-Luo Jiang, Bartosz Szczesny, Alastair M Rucklidge, and Matjaž Perc. Cyclic dominance in evolutionary games: a review. *Journal of the Royal Society Interface*, 11(100):20140735, 2014.
- [23] Tobias Reichenbach, Mauro Mobilia, and Erwin Frey. Mobility promotes and jeopardizes biodiversity in rock–paper–scissors games. *Nature*, 448(7157):1046–1049, 2007.
- [24] Robert M May and Warren J Leonard. Nonlinear aspects of competition between three species. *SIAM journal on applied mathematics*, 29(2):243–253, 1975.
- [25] Tobias Reichenbach, Mauro Mobilia, and Erwin Frey. Self-organization of mobile populations in cyclic competition. *Journal of Theoretical Biology*, 254(2):368–383, 2008.
- [26] Qian He, Mauro Mobilia, and Uwe C Täuber. Spatial rock-paper-scissors models with inhomogeneous reaction rates. *Physical Review E*, 82(5):051909, 2010.
- [27] CM Postlethwaite and AM Rucklidge. Spirals and heteroclinic cycles in a spatially extended rock-paper-scissors model of cyclic dominance. *EPL (Europhysics Letters)*, 117(4):48006, 2017.
- [28] Bartosz Szczesny, Mauro Mobilia, and Alastair M Rucklidge. When does cyclic dominance lead to stable spiral waves? *EPL (Europhysics Letters)*, 102(2):28012, 2013.
- [29] Peter D Taylor and Leo B Jonker. Evolutionary stable strategies and game dynamics. *Mathematical Biosciences*, 40(1-2):145–156, 1978.
- [30] E. C. Zeeman. Population dynamics from game theory. In *Global Theory of Dynamical Systems*, number 819 in Springer Lecture Notes in Mathematics. Springer, 1980.
- [31] J. Hofbauer. On the occurrence of limit cycles in the volterra- lotka equation. *Nonlinear Analysis, Theory, Methods and Applications*, 5(9):1003–1007, 1981.
- [32] Immanuel M Bomze. Lotka-volterra equation and replicator dynamics: a two-dimensional classification. *Biological cybernetics*, 48(3):201–211, 1983.
- [33] Yuzuru Sato, Eizo Akiyama, and J. Doyné Farmer. Chaos in learning a simple two-person game. *PNAS*, 99(7):4748–4751, 2002.
- [34] Elisabeth Paulson and Christopher Griffin. Cooperation can emerge in prisoner’s dilemma from a multi-species predator prey replicator dynamic. *Mathematical Biosciences*, 278:56 – 62, 2016.

- [35] K. J. Davies, J.E. F. Green, N. G. Bean, B. J. Binder, and J. V. Ross. On the derivation of approximations to cellular automata models and the assumption of independence. *Mathematical Biosciences*, 254:63–71, 2004.
- [36] Alexander van Oudenaarden. Systems Biology, Chapter X: Diffusion (MIT Lecture Notes). http://web.mit.edu/biophysics/sbio/PDFs/L15_notes.pdf, Fall 2009.
- [37] Richard G Casten and Charles J Holland. Stability properties of solutions to systems of reaction-diffusion equations. *SIAM Journal on Applied Mathematics*, 33(2):353–364, 1977.